

Structure and magnetic properties of multiferroic $\text{YCr}_{1-x}\text{Fe}_x\text{O}_3$ ($0 \leq x \leq 1$)^{*}

S. KOVACHEV^{*}, D. KOVACHEVA^a, S. ALEKSOVSKA^b, E. SVAB^c, K. KREZHOV

Institute for Nuclear Research and Nuclear Energy, Bulgarian Academy of Sciences, 72 Tzarigradsko Chaussee Blvd., 1784 Sofia, Bulgaria.

^a *Institute of General and Inorganic Chemistry, Bulgarian Academy of Science, "Acad. Georgi Bonchev" str. bld. 11, 1113 Sofia, Bulgaria.*

^b *Institute of Chemistry, Faculty of Natural Sciences and Mathematics, University "Sts. Cyril and Methodius", 1000 Skopje, Republic of Macedonia.*

^c *Research Institute for Solid State Physics and Optics, H-1525 Budapest, POB 49, Hungary.*

Samples from the mixed oxide system $\text{YCr}_{1-x}\text{Fe}_x\text{O}_3$ ($0 \leq x \leq 1$) were prepared by self-propagation combustion techniques and studied by neutron and X-ray diffraction at 290 K and by magnetic measurements in the range 2–800 K. The average observed metal-oxygen distances based on refinements in the space group Pnma are in agreement with the expected distances from the valence bond approach. The non-collinear spin arrangement (mode Γ_4) of YFeO_3 and YCrO_3 is preserved for the rest ($x \geq 0.33$) of the compounds magnetic at 290 K. The findings indicate that YCrO_3 and YFeO_3 form a solid solution with strongly frustrated magnetic interactions.

(Received November 5, 2008; accepted December 15, 2008)

Keywords: Multiferroics, ferroelectricity, diffraction, perovskite, solid solution

1. Introduction

In multiferroic materials the magnetic and ferroelectric orderings coexist and are coupled [1]. Beside important implications for novel electronic devices [2], the physics behind the expected complex magnetolectric phenomena is of great current interest [3]. Few multiferroic compounds with effective magnetolectric properties are known (e.g. BiFeO_3 , BiMnO_3 , YMnO_3), since proper ferroelectricity and magnetism are usually antithetic [1,3]. Much of the current interest is in the so-called improper multiferroics (with magnetically induced ferroelectricity) such as RMnO_3 , RMn_2O_5 (R= rare earth) and other perovskite-like materials with frustrated magnetic interactions and non-collinear spin ordering [3,4].

In this paper, the subjects of investigation are mixed oxides Y-Fe-Cr-O ($0 \leq x \leq 1$) whose end members YFeO_3 and YCrO_3 display intriguing magnetic and electric properties (ferroelectric data for YCrO_3 are given in [3]). Previous research work drew attention to the great complexity of the magnetic properties in the system [5-7]. We found the structural information for the system very

limited and undertook a systematic structural and magnetic characterization of phases in the system.

2. Sample preparation

Materials with the general formula $\text{YCr}_{1-x}\text{Fe}_x\text{O}_3$ ($x = 1.0, 0.875, 0.75, 0.67, 0.5, 0.33, 0.25, 0.125, 0.0$) were obtained as polycrystalline powders by implementing a modified self-propagation combustion method [8]. The reaction products were characterized by X-Ray diffraction (XRD) for phase identification and to assess phase purity.

YCrO_3 was synthesized by slow evaporation and self-ignition of a stoichiometric reaction mixture of $\text{Y}(\text{NO}_3)_3 \cdot 5\text{H}_2\text{O}$, $\text{Cr}(\text{NO}_3)_3 \cdot 9\text{H}_2\text{O}$ and an organic component (sucrose – $\text{C}_{12}\text{H}_{22}\text{O}_{11}$). The other members of the series were prepared by the same method, where a stoichiometric amount of $\text{Fe}(\text{NO}_3)_3 \cdot 9\text{H}_2\text{O}$ was added. In contrast to YCrO_3 , the synthesis of $\text{YCr}_{1-x}\text{Fe}_x\text{O}_3$ ($0 < x < 1$) material proceeded without intermediate forming of YCrO_4 .

3. Experimental

^{*} Paper presented at the International School on Condensed Matter Physics, Varna, Bulgaria, September 2008

The X-Ray powder diffraction (XPD) patterns for structural refinement were recorded on a Bruker D8 Advance powder diffractometer (CuK α radiation, SolX energy dispersive detector) in the 10°-130° 2 θ range, with a 0.02° 2 θ step and a counting time of 10 sec/step. Neutron powder diffraction (NPD) patterns (5°-113° in 2 θ , steps of 0.1°, wavelength of 1.065 Å) were measured on the PSD diffractometer at the Budapest Neutron Centre. The crystal and magnetic structure refinements of the XRD and NPD patterns were carried out by the Rietveld method, implemented in the FullProf package [9].

The dc magnetic susceptibility was measured by means of a Faraday-type magnetic balance in the temperature range 300–800 K in a magnetic field of 7 kOe and with a commercial SQUID magnetometer in the temperature range 2–400 K.

4. Results

Fig. 1 shows that the main XRD peaks have nearly equal intensities and angular positions, indicating that similarly to YFeO₃ and YCrO₃ all the members of the system are orthorhombically distorted perovskites. Correspondingly, all spectra could be indexed within the space group Pnma.

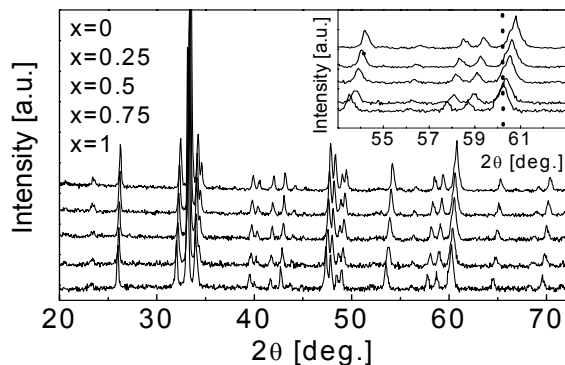


Fig. 1. XRD patterns of the $YCr_{1-x}Fe_xO_3$ series. Inset: limited angular part with reflections 311, 321, 240 and 042.

Fig. 2 presents evidence for long range antiferromagnetic ordering at room temperature in the compositions with $x > 0.25$; neutron diffraction revealed the presence of additional peaks with diffracted intensity depending on Fe-concentration.

Fig. 3 illustrates for YCrO₃ the crystal structure determination from the simultaneous refinement of the XRD and NPD patterns. The structural parameters are set out in Table 1.

The monotonic expansion of the unit cell volume with increasing x matches the refined mean metal-oxygen distances. This can be explained assuming that Fe³⁺ (ionic radius $r_i = 0.645$ Å) substitutes smaller Cr³⁺ ($r_i = 0.615$ Å) [10] and both ions are randomly distributed over the B-sites of the structure. This corroborates the findings for polycrystalline samples with $0.5 \leq x \leq 1$ obtained by solid

state synthesis [7], and the data on single crystals and powders [6]. Remarkably, the lattice constants of our samples, after being treated at 800°C, are close to the values in [7] for samples with similar nominal compositions but heated at temperatures as high as 1350°C.

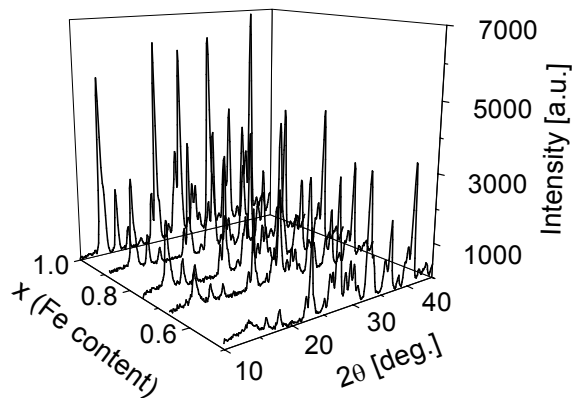


Fig. 2. Low angle part of the room temperature NPD patterns of $YCr_{1-x}Fe_xO_3$.

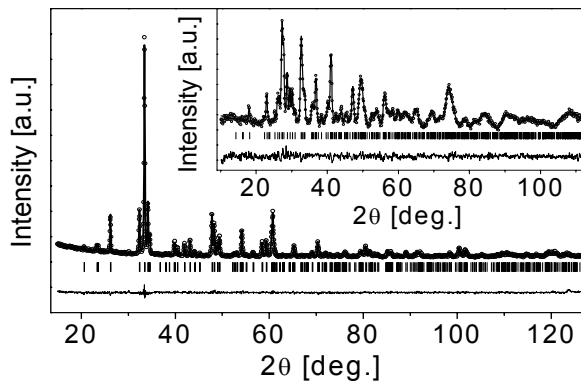


Fig. 3. XRD and NPD (inset) Rietveld plots of $YCrO_3$ at room temperature.

Table 1. Positional and isotropic thermal parameters of $YCrO_3$ (lattice constants in Å: $a = 5.5223(5)$, $b = 7.5338(6)$, $c = 5.2415(4)$).

Ion	x	y	z	B_{iso}
Y ³⁺	0.0663 ₄	0.25	0.9818 ₆	0.55 ₇
Cr ³⁺	0.00	0.00	0.50	0.22 ₈
O ₁ ²⁻	0.464 ₁	0.25	0.106 ₁	0.5 ₁
O ₂ ²⁻	0.1992 ₉	-	0.0537 ₆	0.1953 ₈

The XRD and NPD patterns, as well as the smooth changes in the unit cell volume and measured magnetic

moment versus x depicted in Fig. 4, indicate that the formation of a solid solution of YCrO_3 and YFeO_3 occurs in the whole concentration range. However, the evaluation of the MeO_6 ($\text{Me}=\text{Fe},\text{Cr}$) distortions points to anomalies for $0.33 \leq x \leq 0.67$.

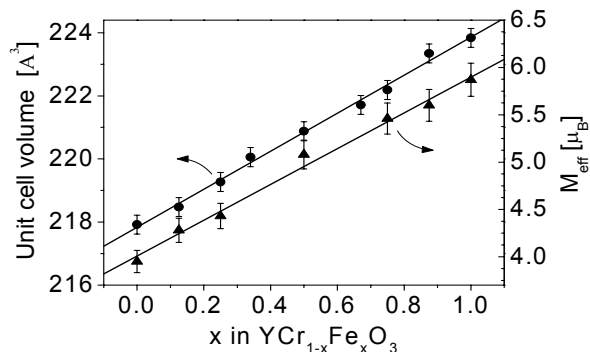


Fig. 4. Dependence of the unit cell volume and the effective magnetic moment on Fe content, x : experimental data with error bars and linear fits

In both YFeO_3 and YCrO_3 below the Neel temperatures $T_N=648\text{K}$ and 141K , respectively, the non-collinear antiferromagnetic state Γ_4 ($G_c F_b A_a$) is established. In this spin arrangement, the basic vector of antiferromagnetism $G=M_1-M_2+M_3-M_4$ (M_i denotes the magnetization of the i -th transition metal ion sublattice) is directed along the c -axis and there is a small admixture of the vector of weak ferromagnetism $F=M_1+M_2+M_3+M_4$ and the vector of weak antiferromagnetism $A=M_1-M_2-M_3+M_4$, which point along the b - and a - crystal axes, respectively. The presence of the constituents F_b and A_a is permitted by crystal symmetry arguments, and their magnitudes are determined mainly by the antisymmetric exchange interaction of Dzialoshinski-Moryia (D-M) between the Fe^{3+} (or Cr^{3+}) ions, which is about two orders of magnitude lower than the isotropic exchange interaction [11]. The D-M interaction is very sensitive to the crystal symmetry and results in the ferromagnetic or antiferromagnetic spin canting.

As exemplified in Fig. 5, we found that the G-type magnetic ordering scheme is preserved for the Fe-rich compositions. Fig. 6 gives a schematic representation of the refined magnetic structures.

In the refinements, Cr atoms (Cr^{3+} spins $S = 3/2$) were allowed to occupy at random the 4b positions together with Fe (Fe^{3+} spins $S = 5/2$), and the complementary occupancy factors were refined, constrained to the full occupancy.

Weak ferromagnetic moment due to the D-M interaction can be easily observed and is well studied [12]. In contrast, the evaluation of A_a is commonly difficult, because of the relatively rather small scattered intensity associated with this magnetic component and spurious effects due to double Bragg reflections when working with

single crystals. Consequently, polarization analysis was needed to overcome the difficulties [13] or to perform careful time of flight neutron scattering experiments [14]. In our YFeO_3 sample, the diffraction peak (021) associated with the weak component A_a was visible. For the patterns in Fig. 2, this and other magnetic components disappear with increasing Cr content, most probably in accordance with the decreasing T_N .

Fig. 7 presents selected plots of the inverse susceptibility and Fig. 8 compares the experimental and calculated Curie constants from the corresponding Curie-Weiss plots, by considering the ideal stoichiometries of the compounds and the commonly used effective magnetic moments of the ions: $\mu_{\text{eff}}(\text{Cr}^{3+}) = 3.8 \mu_B$, $\mu_{\text{eff}}(\text{Fe}^{3+}) = 5.9 \mu_B$ [15].

Fig. 9 demonstrates, for the example of $x=0.33$, the complex behaviour of the magnetization with temperature. Small amounts of Cr in YFeO_3 or Fe in YCrO_3 were found to lead to a considerable decrease in the magnitude of the component F [5,6]. Moreover, in the intermediate concentration interval a partial or full reorientation of the vector F takes place from the c -axis (at high temperature) to the a -axis (at low temperature) [16].

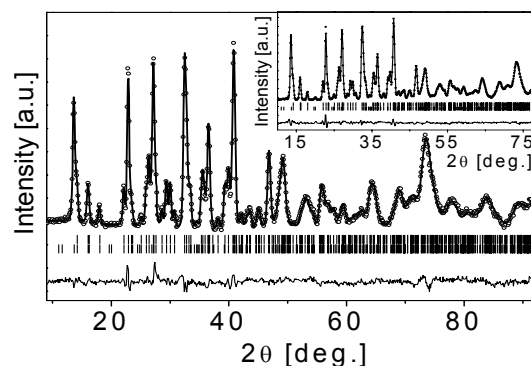


Fig. 5. Room temperature Rietveld plots of $\text{YFe}_{0.875}\text{Cr}_{0.125}\text{O}_3$ and YFeO_3 (inset)

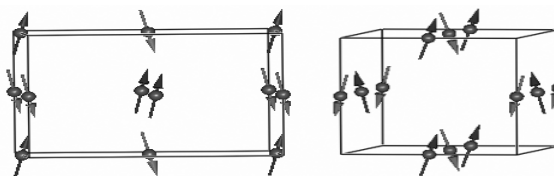


Fig. 6. Schematic view of the magnetic structure at room temperature of $\text{YCr}_{1-x}\text{Fe}_x\text{O}_3$ ($0.33 < x < 1$): (left) along the a -axis, (right) along the b -axis.

The considerations [5,6,16] of the anomalous (for solid solutions) magnetic behaviour came to the

conclusion that the matrix-impurity model fails. Spin glass formation mechanisms could be involved, but our data present additional arguments to those in [7] for discarding such a model, as well.

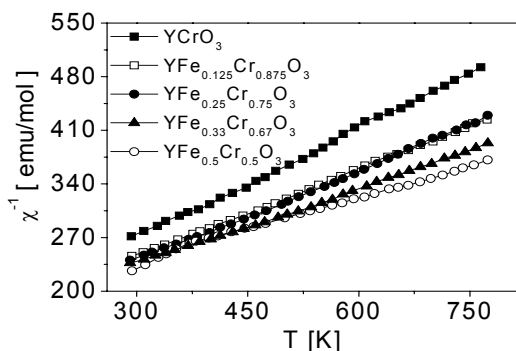


Fig. 7. Dependence of the inverse magnetic susceptibility on temperature for $T > 300$ K for $YCr_{1-x}Fe_xO_3$ ($0 \leq x \leq 0.5$).

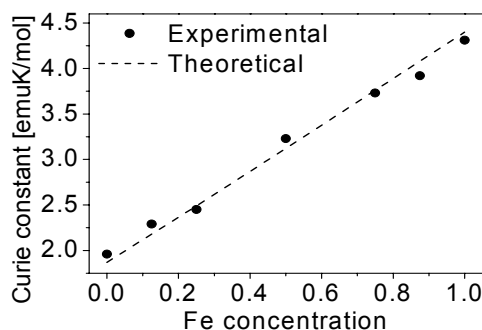


Fig. 8. Curie constant versus Fe concentration x .

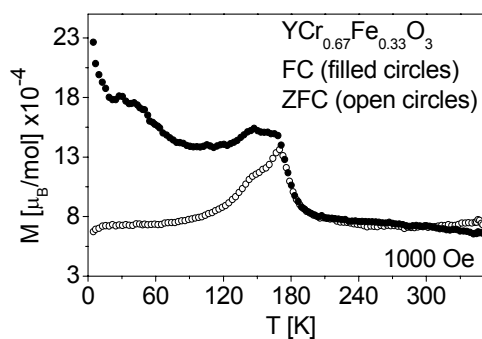


Fig. 9. $x=0.33$: magnetization vs temperature

5. Conclusions

The structural results for $YCr_{1-x}Fe_xO_3$ and the specific thermomagnetic behaviour of the system give a strong indication that replacement of Cr with Fe entails a

substantially modified antisymmetric exchange and frustrated magnetic interactions.

Acknowledgements

This work was supported by the Bulgarian National Fund for Science under Grant No. BM-03/2006, the Hungarian OTKA-T42495 and the European Commission R113-CT-2003-505925.

References

- [1] N. Hill, J. Phys. Chem. B **104**, 6694 (2000).
- [2] T. Lottermoser, T. Lonkai, U. Amann, D. Hohlwein, J. Ihlinger, M. Fiebig, Nature **430**, 541 (2004).
- [3] C. R. Serrao, A. K. Kundu, S. B. Krupanidhi, U. V. Waghmare, C. N. R. Rao, Phys. Rev. B **72**, 220101 (2005).
- [4] A. Moreira dos Santos, A. K. Cheetham, T. Atou, Y. Yamaguchi, K. Ohoyama, H. Chiba, C. N. R. Rao, Phys. Rev. B **66**, 064425 (2002).
- [5] K. Belov, A. Kadomtseva, I. Krynetskii, T. Ovchinnikova, G. Ronami, V. Timofeeva, Sov. Phys. Solid State **14**, 1306 (1972).
- [6] A. Kadomtseva, A. Moskvina, I. Bostrem, B. Wanklyn, N. Khafizova, Sov. Phys. JETP **45**, 1202 (1977).
- [7] A. Dahmani, M. Taibi, M. Noguez, J. Aride, E. Loudghiri, A. Belayachi, Mater. Chem. Phys. **77**, 912 (2002).
- [8] D. Kovacheva, H. Gadjov, K. Petrov, S. Mandal, M. G. Lazarraga, L. Pascual, J. M. Amarilla, R. M. Rojas, P. Herrero, J. M. Rojo, J. Mater. Chem. **12**, 1184(2002).
- [9] J. Rodriguez-Carvajal, T. Roisnel (2006). FullProf, WinPLOTR.
- [10] R. D. Shannon, Acta Cryst. A **32**, 751(1976).
- [11] G. Gorodetsky, D. Treves, Phys. Rev. **135**, A97 (1964).
- [12] A. S. Borovik-Romanov, M. P. Orlova, Sov. Phys. JETP **4**, 531 (1957); A. S. Borovik-Romanov, V. I. Ozhogin, ibid **12**, 18 (1960).
- [13] V. Plakhty, Yu. Chernenkov, J. Schweizer, M. Bedrizova, Sov. Phys. JETP **53**, 1291 (1981).
- [14] D. Georgiev, K. Krezhov, V. V. Nietz, Solid State Commun. **96**, 535(1995).
- [15] A. H. Morrish. The Physical Principles of Magnetism. Wiley, New York (1966), p. 67.
- [16] K. Belov, A. Kadomtseva, T. Ovchinnikova, M. Lukina, M. Pardavi-Horvath, A. Timofeeva, E. Svab, Kristallografiya **21**, 602 (1976).

*Corresponding author: kovachev@gmx.net